On Tanaka-Mura's fatigue crack nucleation model and validation

Wu, Xijia

Publisher's version / Version de l'éditeur:
https://doi.org/10.1111/ffe.12736
Fatigue & Fracture of Engineering Materials & Structures, 2017-10-27

Received: 10 July 2017 | Revised: 1 September 2017 | Accepted: 2 October 2017

DOI: 10.1111/ffe.12736

ORIGINAL CONTRIBUTION

WILEY

On Tanaka-Mura's fatigue crack nucleation model and validation

Xijia Wu

Structures, Materials and Manufacturing Laboratory, Aerospace, National Research Council Canada, 1200 Montreal Rd., Ottawa, ON K1A 0R6, Canada

Correspondence
Xijia Wu, Structures, Materials and Manufacturing Laboratory, Aerospace, National Research Council Canada, 1200 Montreal Rd., Ottawa, ON K1A 0R6, Canada.
Email: xijia.wu@nrc-cnrc.gc.ca

Abstract

Tanaka-Mura's fatigue crack nucleation model is revisited. A dimensional problem is found in their cyclic plastic strain formulation obtained by integration of the displacement function, and hence, it is rederived based on the true strain definition. Using the corrected strain formulation, a new fatigue crack nucleation life expression is obtained, and for the first time, low cycle fatigue lives of several metals and alloys are predicted without resorting to experiments. With such theoretical life as the baseline, other factors such as surface roughness, environment, and even high-temperature damage mechanisms can be delineated in further studies.

KEYWORDS

dislocations, fatigue crack nucleation, fatigue life prediction

1 | INTRODUCTION

Fatigue failure has been studied crossing two centuries, since Wöhler[1] in 1867, which has been understood to be a process consisting of crack nucleation and propagation. In the 1950s, Coffin and Manson independently found through experiments that[2,3]

$$\frac{\Delta\varepsilon_p}{2} = \varepsilon_f N_c{}^c, \tag{1}$$

where ε_f is the material's fatigue ductility and c is a power-index falling in a narrow range of −0.45 to −0.65 for most metals and alloys. This finding links fatigue life to cyclic plasticity via slip, which is also supported by metallurgical studies.[4] But engineers have to perform fatigue tests to determine the fatigue ductility constant for each material ever studied.

Nomenclature: a, half grain size; b, Burgers vector; w_s, γ_{SV}, surface energy; S_{SV}, entropy; μ, shear modulus; ν, Poisson's ratio; τ, shear stress; γ, shear strain; ε, normal strain; ε_f, fatigue ductility in Coffin-Manson relationship; k, frictional stress; $D_1(x)$, dislocation density; U, plastic strain energy; R_s, surface roughness factor

In 1981, Tanaka and Mura developed a theoretical fatigue crack nucleation model in terms of continuously distributed dislocation dipole pile-ups with the crack nucleation life as given by (eqs. 35 and 36 in Tanaka and Mura[5])

$$N_c = \frac{4\pi(1-\nu)w_s a^3}{\mu}\Delta\gamma^{-2}, \tag{2}$$

or, in terms of stress, as

$$N_c = \frac{4\mu w_s}{\pi(1-\nu)a}(\Delta\tau - 2k)^{-2}, \tag{3}$$

where w_s is the surface energy, μ is shear modulus, ν is Poisson's ratio, k is friction stress, and a is half grain size.

This model receives its popularity because it captures the essence of crack nucleation via dislocation slip and predicates the dependence of fatigue crack nucleation life N_c on the cyclic plastic strain range $\Delta\gamma$ with a power-exponent—½, which agrees with the Coffin-Manson relationship. However, the strain-based version (Equation 2) is rarely used in practice, because in Tanaka-Mura's original model, $\Delta\gamma$ bears a physical dimension of $[m]^2$ (see the next section for details), which cannot be experimentally

determined from strain measurements. If the true strain were used in Equation 2, one would find an additional physical dimension of $[m]^4$ on the right-hand side of the equation, which would not be correct. Actually, the stress-based version (Equation 3) is most often used in engineering analyses for real materials.[6-9] But, in those analyses, the surface energy w_s is often termed as the "specific fracture energy" that is often given arbitrary values (other than independently assessed) to fit the fatigue curve, eg, in Tryon and Cruse,[6] $w_s = 440$ kJ/m^2 for stainless steel, and in other works,[7-9] $w_s = 2$ kJ/m^2 for a martensitic steel. These values are orders-of-magnitude higher than the surface energies of metals, reported by Tyson and Miller.[10] Besides, the lattice friction stress k is also difficult to estimate from stress-strain measurements on material coupons. Therefore, in a physically rigorous sense, Equations 2 and/or 3 have never been experimentally validated.

In this paper, we will revisit Tanaka-Mura's model and correct the dimensional problem borne with their original derivation of Equation 2. Then we will proceed to validate the corrected model by comparison with experimental fatigue properties of pure metals and alloys. In the evaluation, nothing but material physical properties, w_s, μ, ν, and b, are used.

2 | TANAKA-MURA'S MODEL REVISITED

Taking the same premise of Tanaka-Mura's model, two-layer inverted dislocation pile-ups are assumed to form along the slip plane, as shown in Figure 1. The first dislocation pile-up forms on layer I during loading, and on reverse loading, instead of these pile-up dislocations moving back on the original pile-up plane, they exert forces to induce dislocation pile-up of opposite sign on another layer, layer II, which is very close to layer I. Such configuration of dislocation pile-ups constitutes either (1) vacancy dipoles, (2) interstitial dipoles, or (3) a combination of both, eg, tripoles. Without further digressing in words, we follow Tanaka-Mura's mathematical derivation to the point where they made the mistake.

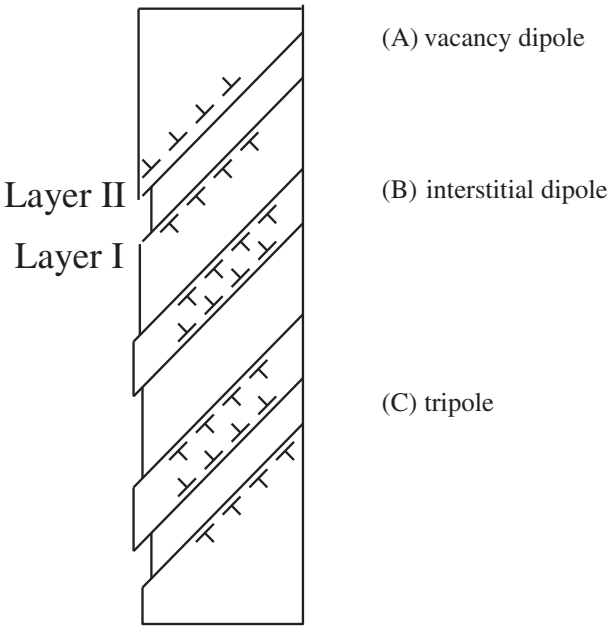

FIGURE 1 Dislocations in A, vacancy dipoles (forming an intrusion); B, interstitial dipoles (forming an extrusion); and C, tripoles (forming an intrusion-extrusion pair) at the surface

Under the first loading of stress τ_1 greater than the frictional stress k, the dislocation density $D_1(x)$ is produced on layer I, satisfying the force-balance equation:

$$\int_{-a}^{a} \frac{\mu b D_1(\xi) d\xi}{2\pi(1-\nu)(x-\xi)} + \tau_1 - k = 0, \tag{4}$$

where b is the Burgers vector and k is the friction stress. Note that integration over the negative range corresponds to the imaginary part of the pile-up beyond the free surface. Using the Muskhelishvili's inversion formula, Equation 4 is solved to yield

$$D_1(x_1) = \frac{2(1-\nu)(\tau_1-k)}{\mu b} \frac{x}{\sqrt{a^2-x^2}}. \tag{5}$$

Note that the dislocation distribution is asymmetrical about $x = 0$. This is typical of Bilby-Cottrell-Swinden distribution with equal number but opposite sign of dislocations distributed on the two sides, which would lead to formation of a center crack or a surface edge crack (with half of the configuration for real).

The total number of dislocations between $x = 0$ and a is (eq. 5 in Tanaka and Mura[5])

$$N_1 = \int_0^a D_1(x')dx' = \frac{2(1-\nu)(\tau_1-k)a}{\mu b}. \tag{6}$$

The plastic displacement caused by the motion of dislocations is given by the integral (eq. 5a in Tanaka and Mura[5])

$$\Phi(x) = \int_x^a b D_1(x')dx'. \tag{7}$$

In Tanaka-Mura's model, the "total plastic displacement" (later called "plastic strain") is calculated by (eq. 6 in Tanaka and Mura[5])

$$\gamma_1 = \int_{-a}^{a} \Phi(x)dx = \int_{-a}^{a} b D_1(x')xdx' = \frac{\pi(1-\nu)(\tau_1-k)a^2}{\mu}. \tag{8}$$

Note that Equation 8 is actually integration of displacement, which results in a dimension of $[m]^2$. Therefore, the physical meaning and dimension of γ_1 as either "the total plastic displacement" or "strain" is incorrect!

By definition, strain is displacement over the distance it is measured. In this case, the slip distance is evaluated as the number of dislocations (given by Equation 6) times the Burgers vector, ie, $\Delta l = N_1 b$, which occurs over distance a. Thus, the plastic strain due to the dislocation pile-up should be equal to $N_1 b/a$, or given by the integral:

$$\gamma_1 = \frac{1}{a}\int_0^a bD_1(x)dx = \frac{2(1-\nu)(\tau_1 - k)}{\mu}. \quad (9)$$

The rest still follows Tanaka-Mura's derivation, except the strain expression. Then the stored energy associated with the dislocation pile-up on layer I is calculated to be

$$U^{(1)} = \frac{1}{2}(\tau_1 - k)\gamma_1. \quad (10)$$

On loading reversal, another pile-up occurs in layer II, satisfying

$$\int_{-a}^{a} \frac{\mu b D_2(\xi)d\xi}{2\pi(1-\nu)(x-\xi)} + \int_{-a}^{a} \frac{\mu b D_1(\xi)d\xi}{2\pi(1-\nu)(x-\xi)} + \tau_2 + k = 0. \quad (11)$$

The distribution function for the pile-up in layer II is thus given by

$$D_2(x) = -\frac{2(1-\nu)(\Delta\tau - 2k)}{\mu b}\frac{x_1}{\sqrt{a^2 - x^2}}, \quad (12)$$

where $\Delta\tau = \tau_1 - \tau_2$ is the stress range.

The plastic strain associated with the pile-up in layer II is given by

$$\gamma_2 = \frac{1}{a}\int_0^a bD_2(x)dx = -\frac{2(1-\nu)(\Delta\tau - 2k)}{\mu}. \quad (13)$$

And hence, the stored energy associated with the dislocation pile-up in layer II is given by

$$U^{(2)} = \frac{1}{2}(\Delta\tau - 2k)\gamma_2. \quad (14)$$

On the k-th reversal, the dislocation distribution $D_k(x)$, the strain γ_k, and the stored energy $U^{(k)}$ are obtained in a similar manner:

$$D_k(x) = (-1)^{k+1}\frac{2(1-\nu)(\Delta\tau - 2k)x}{\mu\sqrt{a^2 - x^2}}, \quad \gamma_k = (-1)^{k+1}\Delta\gamma, \quad U^{(k)} = \Delta U, \quad (15)$$

where

$$\Delta\gamma = \frac{2(1-\nu)(\Delta\tau - 2k)}{\mu}, \quad (16)$$

$$\Delta U = \frac{1}{2}(\Delta\tau - 2k)\Delta\gamma. \quad (17)$$

The index k takes 2N at the minimum and 2N + 1 at the maximum stress after N cycles.

By the Griffith energy criteria, the entire pile-up bursts into a crack once the stored energy in the material volume (ba) becomes equal to the energy to form new crack surfaces ($2a$) (eq. 34 in Tanaka and Mura[5]):

$$N\,\Delta U b a = 2a w_s, \quad (18)$$

where w_s is the surface energy per unit area.

Then the number of cycles to crack nucleation can be obtained, by substituting Equation 17 into Equation 18, as

$$N_c = \frac{2\mu w_s}{b(1-\nu)(\Delta\tau - 2k)^2}. \quad (19)$$

Or, in terms of plastic strain,

$$N_c = \frac{8(1-\nu)w_s}{\mu b}\frac{1}{\Delta\gamma^2}. \quad (20)$$

The most striking difference between Equations 20 and Equation 2 is that Equation 2 obtained by Tanaka and Mura contains extra terms of ba^3. Unless strain could be measured with a dimension of $[m]^2$, Equation 2 cannot be used directly for fatigue life analysis. Comparing Equation 19 to Equation 3, Equation 19 asserts that the fatigue life is proportional to w_s/b instead of w_s/a as given by Equation 3, despite that there may be a Hall-Petch–type relationship for k. Now, we have shown that the extra grain-size dependence in Tanaka-Mura's original model was introduced by evaluation of strain from the displacement integration. It is also shown that the final derived formulations (Equations 19 and 20) do not depend on what a really is, which means a can be the length of any region where persistent slip band spreads, be it within a

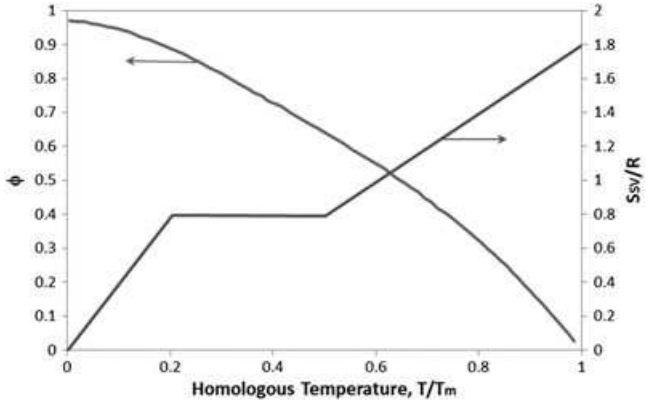

FIGURE 2 Variation of surface free energy and entropy with homologous temperature, after Tyson and Miller[10]

TABLE 1 Values of surface energy and RT_m/A

Element	γ_{SV} (J/m^2)	RT_m/A (J/m^2)
Ag	1.086	0.160
Al	1.020	0.123
Au	1.333	0.173
B	1.060	~0.55
Ba	0.326	0.054
Be	1.298	0.330
Bi	0.446	0.043
Ca	0.425	0.077
Cd	0.696	0.066
Co	2.218	0.304
Cr	2.006	0.348
Cs	0.084	0.011
Cu	1.566	0.224
Fe	2.123	0.294
Ga	0.845	0.036
Ge	0.748	0.129
Hf	1.923	0.270
Hg	0.580	0.025
In	0.658	0.042
Ir	2.658	0.393
K	0.129	0.016
Li	0.472	0.050
Mg	0.688	0.097
Mn	1.298	0.245
Mo	2.510	0.397
Na	0.234	0.027
Nb	2.314	0.342
Nd	0.812	0.090
Ni	2.080	0.300
Os	2.950	0.489
Pb	0.540	0.053
Pd	1.743	0.260
Pt	2.203	0.286
Rb	0.104	0.013
Re	3.133	0.493
Ru	2.655	0.388
Rh	2.325	0.334
Sb	0.461	0.136
Si	0.940	0.195
Sn	0.661	0.048
Sr	0.358	0.061
Ta	2.493	0.409
Ti	1.749	0.240
Tl	0.550	0.052
U	1.780	0.159
V	2.301	0.321
W	2.765	0.500
Zn	0.896	0.097
Zr	1.687	0.222

single fine grain in a polycrystalline material or a large single-crystal industrial turbine blade.

To physically validate the model, in this paper, we shall proceed with the strain-based version (Equation 20) since both the fatigue life N_c and plastic strain range $\Delta\gamma$ are observable quantities, and the w_s, μ, and b are known material properties and parameters, at least for pure metals.

3 | DISCUSSION

Tyson and Miller have obtained the surface energies for a number of pure metals.[10] The surface energy γ_{SV} (=w_s) at temperature T is given by the following equation:

$$\gamma_{SV} - \gamma_{SV}(T_m) = \int_T^{T_m} \frac{S_{SV}}{A} dT = \varphi(T)\frac{RT_m}{A}, \qquad (21)$$

where $\gamma_{SV}(T_m)$ is the surface energy at the melting temperature and A is the surface area per mole of surface atoms. The variations of entropy S_{SV} and ϕ with the homologous temperature, T/T_m, are shown in Figure 2. The values of $\gamma_{SV}(T_m)$ and RT/A for a number of pure elements are given[10] in Table 1.

In practice, fatigue life is assessed through testing of coupons with certain surface finish by machining. We generally apply a surface roughness factor R_s to accommodate the effect of surface roughness such that for real engineering test coupons, $w'_s = R_s w_s$ replaces w_s in Equation 20, as

$$N_c = \frac{8(1-\nu)R_s w_s}{\mu b} \frac{1}{\Delta\gamma^2}. \qquad (22)$$

For example, low cycle fatigue (LCF) lives of type 316 stainless steel with different surface finish are shown in Figure 3. The theoretical prediction of Equation 20 exactly

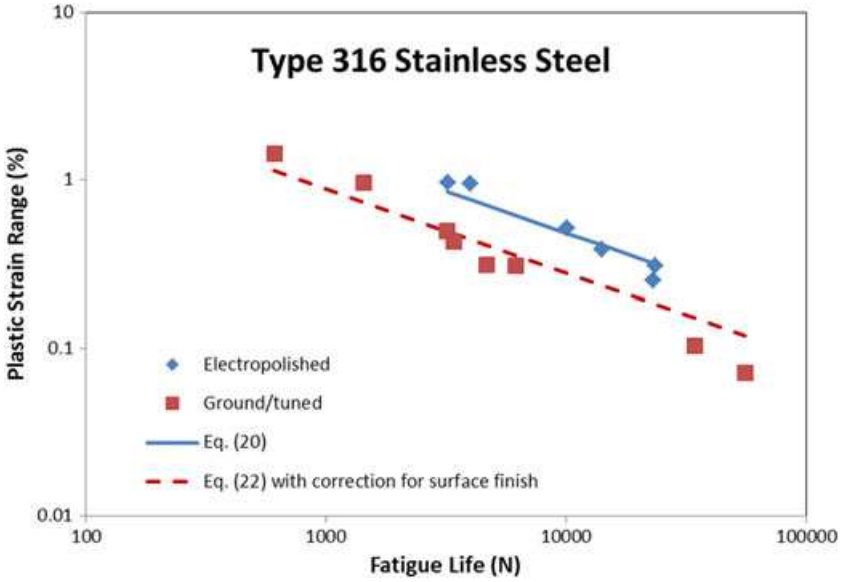

FIGURE 3 Fatigue life of type 316 stainless steel with different surface finish. The symbols represent experimental data taken from Wareing and Vaughan.[11] The lines represent theoretical predictions of Equation 22 [Colour figure can be viewed at wileyonlinelibrary.com]

matches the experimental data for the electropolished surface obtained from Wareing and Vaughan,[11] which represents an "ideal" case. By comparison, the machined surface roughness has an effect of $R_s \sim 1/3$.

Uniaxial LCF life vs plastic strain relations for several metals and alloys at room temperature are evaluated using Equation 22 as shown in Figure 4. For these cases, the homologous temperature is ~0.25, $\phi = 0.85$, $\gamma = \sqrt{3}\varepsilon$, and $R_s = 1/3$ (assuming the same machined condition). The material property parameters and the calculated values of the fatigue life coefficient are given in Table 2; all materials are assumed to have a Poisson's ratio of 0.3. The theoretical predictions of Equation 22 are in very good agreement with experimental data for type 316 stainless steel,[11] copper,[12] titanium,[13] tungsten,[14] Ni-base superalloy—Waspaloy,[15] and Co-base superalloy—Mar-M 509.[16] As shown in Figure 4, the fatigue lifelines for different metals are not far apart. For Waspaloy, data from coarse-grained (CG) microstructure with the grain size of 125 μm and fine-grained (FG) microstructure with the grain size of 16 μm do not show much difference either in the LCF life vs plastic strain plot. Actually, Mughrabi and Höppel also compared the fatigue life of conventional grain-size Cu and ultra-fine grain size Cu, the correlation with plastic strain range also fall within

TABLE 2 Calculation of fatigue coefficient for a number of metals/alloys

Material and reference	E, GPa	b, 10^{-10} m	$\frac{8(1-\nu)R_s w_s}{3\mu b}$
Cu[12]	112	2.56	0.099
Ti[13]	54.5	3.21	0.181
W[14]	286	2.74	0.066
Fe (type 316 stainless steel[11])	199	2.48	0.117
Ni (Waspaloy[15])	211	2.48	0.072
Co (Mar-M 509[16])	211	2.48	0.077

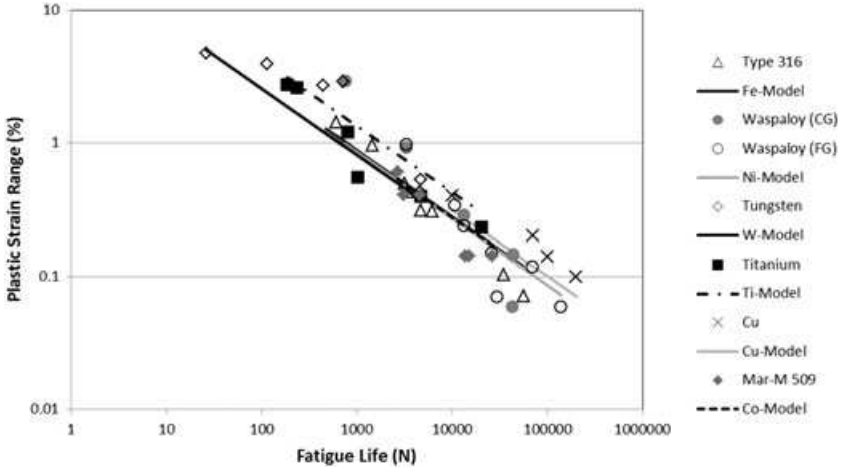

FIGURE 4 Predicted fatigue curves in comparison with experimental data

the factor-of-two bands, not as large as implied by Equation 2 ($\sim a^3$). In terms of stress, however, the Hall-Petch effect of grain size as well as precipitates may affect the lattice friction resistance k such that the relationship (Equation 19) may indeed be affected by the microstructure. Also, in alloys, solute atoms may have an effect on the surface energy, as compared to the pure metal. In that case, surface energy containing solute atoms (at. %) needs to be evaluated. Microstructural and alloying effects need to be further studied, but it is beyond the scope of the present paper.

4 | CONCLUSION

A fatigue crack nucleation model is developed by correcting the dimensional error in Tanaka-Mura's original treatment, based on inverted dislocation pile-ups. The validation against experimental data on many engineering materials ranging from bcc to fcc and hcp metals demonstrates that the physical basis of Tanaka-Mura's model is viable, representing fatigue damage in metals. For the first time, LCF lives of metals and alloys are predicted without resorting to experiments, which means that Equation 20 can at least be used to guide design of new materials for the first approximation. With such theoretical life as the baseline, other factors such as surface roughness, environment, and even high-temperature damage mechanisms can be delineated for further study.

ORCID

Xijia Wu http://orcid.org/0000-0002-0250-112X

REFERENCES

1. Wohler A. Editor's notes: Wohler's experiments on the strength of metals. *Engineering*. 1867;4:160-161.
2. S.S. Manson (1954) Behaviour of materials under conditions of thermal stress. National Advisory Commission on aeronautics report TN-2933, Lewis Flight Propulsion Laboratory, Cleveland, OH.
3. Coffin LF. A study of the effects of cyclic thermal stresses on a ductile metal. *Transactions of the American Society of Mechanical Engineers*. 1954;76:931-950.
4. Thompson N, Wadsworth NJ, Louat N. The origin of fatigue fracture in copper. *Phil Mag*. 1956;1:113-126.
5. Tanaka K, Mura YA. A dislocation model for fatigue crack initiation. *J Appl Mech*. 1981;48:97-103.
6. R.G. Tryon and T.A. Cruse (1999) Reliability-based micromechanical small crack growth model. AIAA/ASME/ASCE/AHS/ASC Structures, Structural Dynamics, and Materials Conference, April 1999, St. Louis, MO., USA.
7. Kramberger J, Jezernik N, Goncz P, Glodež S. Extension of the Tanaka-Mura model for fatigue crack initiation in thermally cut martensitic steels. *Eng Fract Mech*. 2010;77:2040-2050.
8. Bruckner-Foit A, Huang X. On the determination of material parameters in crack initiation laws. *Fatigue Fract Eng Mater Struct*. 2008;31:980-988.
9. Jezernik N, Kramberger J, Lassen T, Glodež S. Numerical modelling of fatigue crack initiation and growth of martensitic steels. *Fatigue Fract Eng Mater Struct*. 2010;33:714-723.
10. Tyson WR, Miller WA. Surface free energies of solid metals: estimation from liquid surface tension measurements. *Surf Sci*. 1977;62:267-276.
11. J. Wareing and H.G. Vaughan (1979) Influence of surface finish on low-cycle fatigue characteristics of type 316 stainless steel at 400°C. Metal Science January, 1–8.
12. Mughrabi H, Höppel HW. Cyclic deformation and fatigue properties of very fine-grained metals and alloys. *Int J Fatigue*. 2010;32:1413-1427.
13. Zhang ZF, Gu HC, Tan XL. Low-cycle fatigue behaviours of commercial-purity titanium. *Mater Sci & Eng*. 1998;A252:85-92.
14. Schmunk RE, Korth GE. Tensile and low-cycle fatigue measurements on cross-rolled tungsten. *J Nuclear Mater*. 1981;103&104:943-948.
15. Lerch BA, Jayaraman NA. Study of fatigue damage mechanisms in Waspaloy from 25 to 800°C. *Mater. Sci. & Eng*. 1984;66:151-166.
16. Reuchet J, Remy L. High temperature low cycle fatigue of MAR-M 509 superalloy. *Mater. Sci. & Eng*. 1983;58:19-32.

How to cite this article: Wu X. On Tanaka-Mura's fatigue crack nucleation model and validation. *Fatigue Fract Eng Mater Struct*. 2017;1–6. https://doi.org/10.1111/ffe.12736